



Cite this: *Dalton Trans.*, 2016, **45**, 2208

Hydrophosphination reactions with transition metal ferrocenylphosphine complexes†

Julian Rodger Frederic Pritzwald-Stegmann, Peter Lönnecke and Evamarie Hey-Hawkins*

The group 6 metal mono-, bis- and tris-ferrocenylphosphine complexes $[M(CO)_5(PH_2Fc)]$ (**1a**, M = Cr; **1b**, M = Mo; **1c**, M = W), *cis*- $[M(CO)_4(PH_2Fc)_2]$ (**2a**, M = Cr; **2b**, M = Mo; **2c**, M = W) and *fac*- $[M(CO)_3(PH_2Fc)_3]$ (**3a**, M = Cr; **3b**, M = Mo; **3c**, M = W) [Fc = $Fe(\eta^5-C_5H_4)(\eta^5-C_5H_5)$] were prepared and fully characterised. IR and NMR spectroscopy and single-crystal X-ray diffraction analysis indicate that $FcPH_2$ is as good a σ donor as $PhPH_2$ but is easier to handle and furthermore has a redox-active ferrocenyl group. Complex **1c** was employed in the hydrophosphination of acrylonitrile and methyl acrylate in the presence of catalytic amounts of $KOtBu$ giving the secondary phosphine complexes $[W(CO)_5(PH(Fc)(CH_2CH_2CN))]$ (**4a**) and $[W(CO)_5(PH(Fc)(CH_2CH_2C(O)OMe))]$ (**4b**). In addition, $FcP(CH_2CH_2CN)_2$ (**5**) was prepared by a similar method from $FcPH_2$ and acrylonitrile. These hydrophosphination products represent a convenient method for the modification of phosphines.

Received 31st August 2015,
Accepted 3rd November 2015

DOI: 10.1039/c5dt03374h

www.rsc.org/dalton

Introduction

The majority of organometallic phosphine complexes involve mono-, bi- or polydentate tertiary phosphines,¹ while primary and secondary phosphines have received much less attention, due to their toxicity and high reactivity (some are even pyrophoric). However, these phosphines are very interesting, as they facilitate post-coordination modification of the P–H bond, allowing for chemical flexibility in the synthesis of new and intriguing transition metal phosphine complexes.^{2,3} Several air-stable primary and secondary phosphines have been reported;^{4–10} developments in this area include the use of bulky aryl groups^{7,8} or aminoalkyl substituents.⁹ A recent review by Higham *et al.* gives an excellent overview on primary phosphine chemistry, including air-stable phosphines.³

Due to the redox properties of the ferrocenyl unit and the possibility to readily obtain chiral compounds,¹¹ ferrocenylphosphines are an important class of ligands in transition metal chemistry.^{11,12} Henderson *et al.*^{4–6} used the methylferrocenyl fragment to stabilise primary phosphines. $FcCH_2PH_2$ [Fc = $Fe(\eta^5-C_5H_4)(\eta^5-C_5H_5)$] proved to be indefinitely air-stable,⁶ probably due to electronic rather than steric effects,

as well as having the ability to coordinate to molybdenum carbonyls or $[RuCl_2(p\text{-cymene})_2]$ (*p*-cymene = 1-Me-4-*i*PrC₆H₄) without alteration of the PH₂ group, whereas P–H activation occurred in the reaction with $[Ru_3(CO)_{12}]$ to give two products with capping phosphinidene ligands.⁵ Ferrocenylphosphine, $FcPH_2$, was first published by Roesky *et al.* in 1989 as an air-sensitive yellow oil prepared by reduction of $FcPCL_2$ with $LiAlH_4$.¹³ Henderson *et al.* have obtained $FcPH_2$ from the reduction of $FcP(O)(OEt)_2$ with a mixture of $LiAlH_4$ and Me_3SiCl as a brown oil that crystallises upon standing.⁴ They reported that a solution of $FcPH_2$ is slowly oxidised in 5 d to the corresponding primary phosphine oxide and phosphinic acid.⁴ We have previously extended this chemistry to the sterically demanding air-stable secondary and tertiary ferrocenylphosphines $PH(CH_2Fc)_2$ and $P(CH_2Fc)_3$ ¹⁴ and transition metal complexes thereof.^{14,15–19}

$FcPH_2$ is a remarkably convenient starting material considering its easy synthesis and stability compared with related compounds, but has mostly been neglected. In contrast, the highly reactive $PhPH_2$ has been used extensively.²⁰ We have previously reported the synthesis of $[MI_2(CO)_3(PH_2Fc)_2]$ (M = Mo, W),¹⁹ $[Cp^*TaCl_4(PH_2Fc)]$ ¹⁵ ($Cp^* = C_5Me_5$) and $[RuCl_2(p\text{-cymene})(PH_2Fc)]$.¹⁷ Presented below is the synthesis and characterisation of the ferrocenylphosphine transition metal carbonyl complexes $[M(CO)_5(PH_2Fc)]$ (**1a**, M = Cr; **1b**, M = Mo; **1c**, M = W), *cis*- $[M(CO)_4(PH_2Fc)_2]$ (**2a**, M = Cr; **2b**, M = Mo; **2c**, M = W) and *fac*- $[M(CO)_3(PH_2Fc)_3]$ (**3a**, M = Cr; **3b**, M = Mo; **3c**, M = W). Furthermore, the reactivity of the P–H bond of the coordinated and free ligand in the hydrophosphination of alkenes was investigated, and the hydrophosphination

Institute of Inorganic Chemistry, Faculty of Chemistry and Mineralogy, Universität Leipzig, Johannisallee 29, 04103 Leipzig, Germany. E-mail: hey@uni-leipzig.de

† Electronic supplementary information (ESI) available: Experimental and simulated ¹H and ³¹P NMR spectra of **2a** and **3a** (only PH₂ region); summary of data collection, structure solution and refinement details for **1a,c**, **2a–c**, **3a,b** and **4a**. CCDC 1420127–1420134. For ESI and crystallographic data in CIF or other electronic format see DOI: 10.1039/c5dt03374h



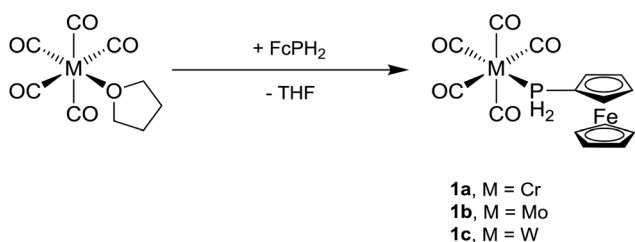
products $[\text{W}(\text{CO})_5\{\text{PH}(\text{Fc})(\text{CH}_2\text{CH}_2\text{CN})\}]$ (**4a**), $[\text{W}(\text{CO})_5\{\text{PH}(\text{Fc})(\text{CH}_2\text{CH}_2\text{C}(\text{O})\text{OMe})\}]$ (**4b**) and $\text{FcP}(\text{CH}_2\text{CH}_2\text{CN})_2$ (**5**) were obtained.

Results and discussion

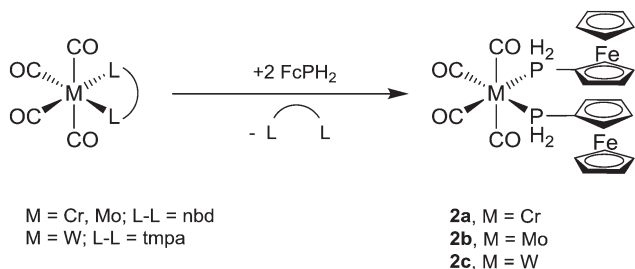
Synthesis

Freshly prepared $[\text{M}(\text{CO})_5(\text{thf})]$ ($\text{M} = \text{Cr}, \text{Mo}, \text{W}$)²¹ was added to a solution of FcPH_2 ³ in THF at room temperature and the mixture was stirred for 30 min (Scheme 1). All volatile materials including unconsumed $\text{M}(\text{CO})_6$ and FcPH_2 were removed under high vacuum (10^{-3} mbar) at elevated temperature to leave a pale orange powder of crude $[\text{M}(\text{CO})_5(\text{PH}_2\text{Fc})]$ (**1a**, $\text{M} = \text{Cr}$; **1b**, $\text{M} = \text{Mo}$; **1c**, $\text{M} = \text{W}$), which was purified by column chromatography. Small amounts of *cis*- $[\text{M}(\text{CO})_4(\text{PH}_2\text{Fc})_2]$ (**2a**, $\text{M} = \text{Cr}$; **2b**, $\text{M} = \text{Mo}$; **2c**, $\text{M} = \text{W}$) were also obtained by this method, since *cis*- $[\text{M}(\text{CO})_4(\text{thf})_2]$ is a side product in the preparation of $[\text{M}(\text{CO})_5(\text{thf})]$.²¹ The three complexes **1a–c** are air- and moisture-stable and highly soluble in common organic solvents.

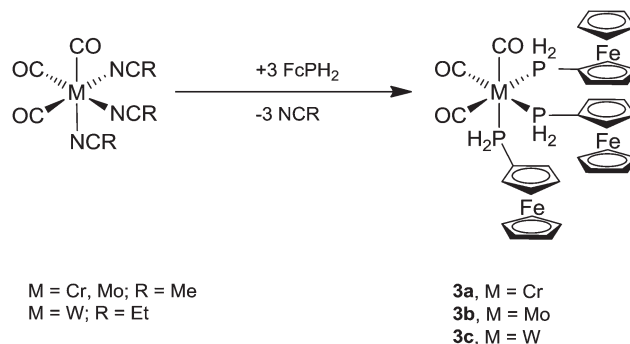
The bis-ferrocenylphosphine complexes *cis*- $[\text{M}(\text{CO})_4(\text{PH}_2\text{Fc})_2]$ (**2a**, $\text{M} = \text{Cr}$; **2b**, $\text{M} = \text{Mo}$) were obtained from two equivalents of FcPH_2 and $[\text{M}(\text{CO})_4(\text{nbnd})]$ ²² ($\text{M} = \text{Cr}, \text{Mo}$, nbnd = norbornadiene) in toluene after stirring at room temperature for 24 h (Scheme 2). In the case of *cis*- $[\text{W}(\text{CO})_4(\text{PH}_2\text{Fc})_2]$ (**2c**), a mixture of FcPH_2 and *cis*- $[\text{W}(\text{CO})_4(\text{tmpa})]$ ²² (tmpa = *N,N,N',N'*-tetramethyl-1,3-propanediamine) in toluene was heated to 60 °C for 1 d. Complexes **2a–c** crystallise from dichloromethane/*n*-hexane as pale orange powders.



Scheme 1 Synthesis of $[\text{M}(\text{CO})_5(\text{PH}_2\text{Fc})]$ (**1a**, $\text{M} = \text{Cr}$; **1b**, $\text{M} = \text{Mo}$; **1c**, $\text{M} = \text{W}$).



Scheme 2 Synthesis of *cis*- $[\text{M}(\text{CO})_4(\text{PH}_2\text{Fc})_2]$ (**2a**, $\text{M} = \text{Cr}$; **2b**, $\text{M} = \text{Mo}$; **2c**, $\text{M} = \text{W}$).



Scheme 3 Synthesis of *fac*- $[\text{M}(\text{CO})_3(\text{PH}_2\text{Fc})_3]$ (**3a**, $\text{M} = \text{Cr}$; **3b**, $\text{M} = \text{Mo}$; **3c**, $\text{M} = \text{W}$).

The tris-ferrocenylphosphine complexes *fac*- $[\text{M}(\text{CO})_3(\text{PH}_2\text{Fc})_3]$ (**3a**, $\text{M} = \text{Cr}$; **3b**, $\text{M} = \text{Mo}$; **3c**, $\text{M} = \text{W}$) were obtained from three equivalents of FcPH_2 and *fac*- $[\text{M}(\text{CO})_3(\text{NCR})_3]$ ($\text{M} = \text{Cr}, \text{Mo}$, $\text{R} = \text{Me}$; $\text{M} = \text{W}$, $\text{R} = \text{Et}$)²¹ in dichloromethane overnight at room temperature (Scheme 3). The air- and moisture-stable products were purified by column chromatography.

Spectroscopic data

The $^{31}\text{P}\{^1\text{H}\}$ NMR spectra show a remarkable difference between the three complexes with $\delta(^{31}\text{P})$ observed at progressively lower ppm in the order $\text{Cr} > \text{Mo} > \text{W}$ (**1a**: -47.6 , **1b**: -81.5 and **1c**: -101.8 ppm). In the proton-coupled ^{31}P NMR spectra these singlets split into triplets [$J_{\text{PH}} \approx 334$ Hz (Table 1)]. In addition, the spectrum of **1c** shows ^{31}P - ^{183}W coupling of 221 Hz.

In the ^1H NMR spectra, the signals of the hydrogen atoms of the primary phosphine are shifted downfield from 3.81 ppm in FcPH_2 to 5.27 ppm in **1a**, 5.31 ppm in **1b** and 5.65 ppm in **1c** (J_{HP} increases from 203.6 Hz in FcPH_2 to 333.9 Hz in **1a**, 328 Hz in **1b** and 341.5 Hz in **1c**).

In the $^{13}\text{C}\{^1\text{H}\}$ NMR spectrum, two doublets are observed for the carbonyl carbon atoms (**1a**: 220.4 ppm, $^2J_{\text{CP}} = 7.3$ Hz, 216.1 ppm, $^2J_{\text{CP}} = 13.7$ Hz; **1b**: 208.8 ppm, $^2J_{\text{CP}} = 23.7$ Hz,

Table 1 Selected spectroscopic data for FcPH_2 , **1a–c**, **2a–c**, **3a–c**, **4a,b** and **5**

Compound	$\delta^{31}\text{P}$ (ppm)	$^1J_{\text{PH}}$ (Hz)	$\nu(\text{CO})$ (cm^{-1})
FcPH_2	-144.2	203.6	—
1a	-47.5	333.9	2066, 1946, 1931, 1917
1b	-81.5	328.0	2074, 1950, 1933, 1921
1c	-101.8	341.5	2073, 1935, 1916, 1898
2a	-36.3	333.1	2018, 1922, 1901, 1870
2b	-72.4	326.4	2024, 1901, 1879
2c	-94.2	328.0	2025, 1922, 1898, 1865
3a	-25.9	306.0	1922, 1837
3b	-63.8	307.0	1932, 1842
3c	-82.3	315.0	1938, 1840
4a	-45.4	345.1	2073, 1980, 1916
4b	-42.6	343.0	2071, 1978, 1914, 1738
5	-74.4	—	—



205.0 ppm, $^2J_{CP} = 9.2$ Hz; **1c**: 198.1 ppm, $^2J_{CP} = 22.2$ Hz, 195.9 ppm, $^2J_{CP} = 7.1$ Hz). The doublet with the larger coupling constant is assigned to the single *trans* carbonyl group, since ^{31}P - ^{13}C coupling through multiple bonds is usually greatest when the bonds are linear.²³

The same trends as seen for **1a-c** are also observed for **2a-c** in the ^1H , $^{13}\text{C}\{^1\text{H}\}$, $^{31}\text{P}\{^1\text{H}\}$ and ^{31}P NMR spectra, but the spectra exhibit a higher spin system due to coupling with the second magnetically inequivalent phosphorus atom (the ^1H and ^{31}P NMR spectra of **2a** (experimental and simulated) are shown in Fig. S1 and S2, ESI†). The signals in the ^{31}P NMR spectra of **2a-c** show downfield shifts of roughly 10 ppm compared to **1a-c** (Table 1). The only significant change in the ^1H NMR spectra of **2a-c** compared to **1a-c** is the increased complexity of the signal of the hydrogen atoms attached to the phosphorus atoms due to the apparent $\text{AA}'\text{X}_2\text{X}'_2$ (**2a,b**) or $\text{AA}'\text{MX}_2\text{X}'_2$ (**2c**) spin system. These signals are observed at 5.23 in **2a**, 5.22 in **2b** and 5.53 ppm in **2c**. Accordingly, the $^{13}\text{C}\{^1\text{H}\}$ NMR spectra of **2a-c** show increased complexity due to the second phosphorus atom, but the same downfield shift trend is observed from chromium to tungsten. The greatest change is seen in the carbonyl carbon signals, which become more deshielded (downfield shifts of 3.9 to 6.2 ppm). This deshielding of the carbonyl carbon atoms is accompanied by a decrease in $\nu(\text{CO})$ of the A_1 carbonyl mode (2018–2025 cm^{-1} , Table 1) in the IR spectra of **2a-c** by about 50 cm^{-1} due to increased back-bonding between the d_M and π^* orbitals of the $\text{M}-\text{CO}$ bond, which is due to the presence of the second FcPH_2 ligand.²⁴

Introduction of a third ferrocenylphosphine ligand further increases the complexity of the ^1H , $^{13}\text{C}\{^1\text{H}\}$, $^{31}\text{P}\{^1\text{H}\}$ and ^{31}P NMR spectra ($\text{AA}'\text{A}''\text{X}_2\text{X}'_2\text{X}''_2$ (**3a,b**) or $\text{AA}'\text{A}''\text{MX}_2\text{X}'_2\text{X}''_2$ (**3c**) spin system; the ^1H and ^{31}P NMR spectra of **3a** (experimental and simulated) are shown in Fig. S3 and S4, ESI†). However, the trends seen in the spectra of **2a-c** are also observed in those of **3a-c**. $\delta(^{31}\text{P})$ of **3a-c** is shifted further downfield by about 10 ppm (Table 1). This suggests increasing deshielding of the phosphine with increased substitution. This same deshielding trend is seen between *cis*- $[\text{M}(\text{CO})_4(\text{PH}_2\text{Ph})_2]$ and *fac*- $[\text{M}(\text{CO})_3(\text{PH}_2\text{Ph})_3]$ ($\text{M} = \text{Mo}, \text{W}$; $\text{M} = \text{Mo}$, $\delta(^{31}\text{P})$ is -60.5 and -53.5 ppm; $\text{M} = \text{W}$, $\delta(^{31}\text{P})$ is -80.9 and -72.0 ppm).²⁵ In addition, the $^{31}\text{P}\{^1\text{H}\}$ NMR spectra of the tungsten complexes (**1c**, **2c** and **3c**) show ^{31}P - ^{183}W coupling which decreases from 221.0 Hz in $[\text{W}(\text{CO})_5(\text{PH}_2\text{Fc})]$ (**1c**) to 209.0 Hz in *fac*- $[\text{W}(\text{CO})_3(\text{PH}_2\text{Fc})_3]$ (**3c**). Coupling to the two NMR active ($I = 5/2$) molybdenum isotopes, ^{95}Mo and ^{97}Mo , is only observed for *fac*- $[\text{Mo}(\text{CO})_3(\text{PH}_2\text{Fc})_3]$ (**3b**). In the $^{13}\text{C}\{^1\text{H}\}$ NMR spectra of **3a-c** the signals of the carbonyl carbon atoms are also shifted by about 4 ppm compared to **2a-c**.

Molecular structures

Single-crystal X-ray structure determinations were carried out for **1a**, **1c**, **2a-c**, **3a** and **3b**. Complexes **1a** and **1c** are isostructural, as are complexes **2a-c** and complexes **3a,b**. Therefore, only one representative structure is shown here in each case (**1a** (Fig. 1, Table 2), **2a** (Fig. 2, Table 3), and **3a** (Fig. 3, Table 4). Furthermore, in **2a-c** two symmetry-independent

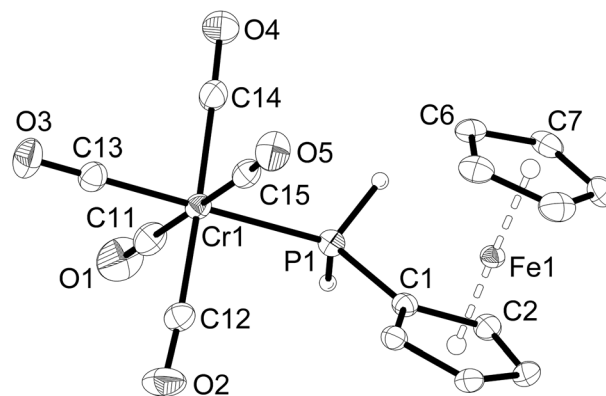


Fig. 1 Molecular structure of $[\text{Cr}(\text{CO})_5(\text{PH}_2\text{Fc})]$ (**1a**). The hydrogen atoms of the ferrocenyl moiety are omitted for clarity. Ellipsoids drawn at 50% probability.

Table 2 Selected bond lengths (pm) and bond angles ($^\circ$) for **1a** and **1c**

Compound	1a (M = Cr)	1c (M = W)
M(1)–P(1)	236.30(3)	251.12(8)
M(1)–C(13)	186.4(1)	201.0(3)
M(1)–C(14)	189.3(1)	204.3(3)
M(1)–C(15)	189.7(1)	203.5(3)
M(1)–C(11)	189.7(1)	204.3(3)
M(1)–C(12)	190.4(1)	205.1(3)
P(1)–C(1)	179.9(1)	180.0(3)
O(1)–C(11)	113.8(2)	113.6(4)
O(2)–C(12)	113.8(2)	113.4(4)
O(3)–C(13)	114.8(2)	114.3(4)
O(4)–C(14)	113.9(2)	113.6(4)
O(5)–C(15)	113.9(2)	113.9(4)
C(13)–M(1)–P(1)	179.06(4)	179.5(1)
C(14)–M(1)–P(1)	90.09(4)	90.6(1)
C(15)–M(1)–P(1)	90.80(4)	90.30(9)
C(11)–M(1)–P(1)	89.17(4)	88.9(1)
C(12)–M(1)–P(1)	91.83(4)	92.13(9)
C(1)–P(1)–M(1)	122.49(4)	121.69(9)

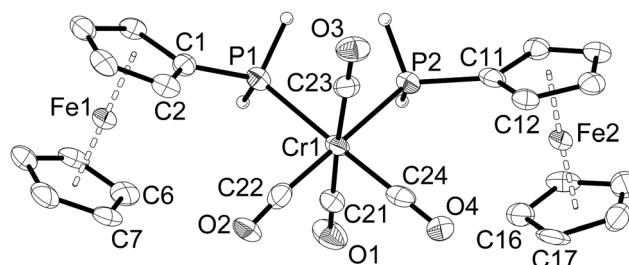


Fig. 2 Molecular structure of *cis*- $[\text{Cr}(\text{CO})_4(\text{PH}_2\text{Fc})_2]$ (**2a**). The hydrogen atoms of the ferrocenyl moieties are omitted for clarity. Ellipsoids drawn at 50% probability. Only one of the symmetry-independent molecules is shown.

molecules are present in the asymmetric unit. As these molecules have very similar structures, only one of the two molecules is shown and discussed. Complexes **3a** and **3b** crystallise



Table 3 Selected bond lengths (pm) and bond angles (°) for **2a–2c**. Values of the second symmetry-independent molecule are given in parentheses †

Compound	2a (M = Cr)	2b (M = Mo)	2c (M = W) ^a
M(1)–P(1)	234.4(3)	250.4(1)	249.3(2)
[M(2)–P(3)]	[234.8(3)]	[250.3(1)]	[249.6(3)]
M(1)–P(2)	235.0(3)	250.2(1)	249.1(2)
[M(2)–P(4)]	[234.4(3)]	[250.3(1)]	[249.2(2)]
M(1)–C(24)	185(1)	198.1(6)	197(1)
[M(2)–C(48)]	[182.7(9)]	[198.1(6)]	[197(1)]
M(1)–C(22)	187(1)	198.8(6)	199(1)
[M(2)–C(46)]	[185(1)]	[199.5(5)]	[198(1)]
M(1)–C(21)	187(1)	204.0(6)	204(1)
[M(2)–C(47)]	[188(1)]	[203.5(5)]	[204(1)]
M(1)–C(23)	189(1)	201.9(5)	198(1)
[M(2)–C(45)]	[188.9(9)]	[204.1(6)]	[201(1)]
P(1)–C(1)	180(1)	180.3(5)	182(1)
[P(3)–C(25)]	[181(1)]	[180.5(5)]	[178.5(9)]
P(2)–C(11)	180(1)	179.7(5)	180(1)
[P(4)–C(35)]	[181(1)]	[181.3(5)]	[180(1)]
C(24)–M(1)–P(1)	178.4(3)	176.9(2)	176.9(3)
[C(48)–M(2)–P(3)]	[178.5(3)]	[178.5(2)]	[178.2(3)]
C(22)–M(1)–P(1)	93.7(3)	94.0(2)	93.0(2)
[C(46)–M(2)–P(3)]	[92.8(3)]	[93.3(1)]	[93.2(3)]
C(21)–M(1)–P(1)	93.1(3)	93.6(2)	93.3(3)
[C(47)–M(2)–P(3)]	[87.1(3)]	[86.5(1)]	[85.8(3)]
C(23)–M(1)–P(1)	87.0(3)	86.7(1)	86.4(3)
[C(45)–M(2)–P(3)]	[88.8(3)]	[89.1(2)]	[88.9(3)]
C(24)–M(1)–P(2)	93.1(3)	92.8(2)	92.8(3)
[C(48)–M(2)–P(4)]	[94.1(3)]	[94.2(2)]	[94.0(3)]
C(22)–M(1)–P(2)	178.8(3)	178.6(2)	178.2(3)
[C(46)–M(2)–P(4)]	[178.4(3)]	[177.6(1)]	[177.5(3)]
C(21)–M(1)–P(2)	89.3(3)	89.0(2)	88.7(3)
[C(47)–M(2)–P(4)]	[87.3(3)]	[86.6(2)]	[86.5(3)]
C(23)–M(1)–P(2)	86.7(3)	86.7(2)	86.6(3)
[C(45)–M(2)–P(4)]	[91.5(3)]	[93.7(2)]	[93.0(3)]
P(1)–M(1)–P(2)	85.7(1)	84.85(4)	84.52(8)
[P(4)–M(2)–P(3)]	[85.7(9)]	[84.88(4)]	[84.69(8)]
C(1)–P(1)–M(1)	122.8(3)	122.6(2)	122.6(3)
[C(25)–P(3)–M(2)]	[124.5(3)]	[124.2(2)]	[123.9(3)]
C(11)–P(2)–M(1)	124.8(3)	124.5(2)	123.9(3)
[C(35)–P(4)–M(2)]	[124.2(3)]	[122.9(2)]	[122.6(3)]

^a As a result of the extremely small and moderately diffracting crystal (small needle), the carbon atoms of **2c** were refined isotropically.

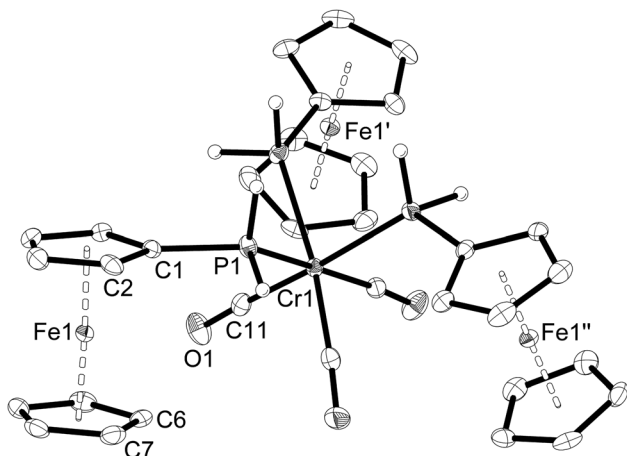


Fig. 3 Molecular structure of *fac*-[Cr(CO)₃(PH₂Fc)₃] (**3a**). The hydrogen atoms of the ferrocenyl moieties are omitted for clarity. Ellipsoids drawn at 50% probability. Symmetry operators: Fe1': 1 – y, 2 + x – y, z; Fe1'': –x + y, 1 – x, z.

Table 4 Selected bond lengths (pm) and bond angles (°) for **3a** and **3b**

Compound	3a (M = Cr)	3b (M = Mo)
M(1)–P(1)	235.15(6)	250.57(7)
P(1)–C(1)	180.5(2)	180.6(2)
M(1)–C(11)	184.9(2)	198.0(3)
C(11)–M(1)–C(11)'	88.0(1)	87.8(1)
C(11)–M(1)–P(1)	172.70(7)	173.64(7)
C(11)'–M(1)–P(1)	87.55(7)	88.50(7)
C(11)''–M(1)–P(1)	97.62(7)	97.22(7)
P(1)–M(1)–P(1)'	87.26(3)	86.83(2)
C(1)–P(1)–M(1)	125.87(7)	125.34(8)

in the trigonal space group *R3* with three molecules in the unit cell. The chirality arises from the lack of rotoinversion symmetry elements in the molecule. The molecules are located on a crystallographic *C*₃ axis.

All complexes retain the octahedral geometry of the parent metal carbonyl complexes with bond angles at the metal centre ranging from 88.0(1) to 92.13(9)° in **1a** and **1c**, but become more distorted with bond angles ranging from 84.5(1)–94.3(4)° in **2a–c**. The most acute angle in **2a–c** is the P–M–P angle, which suggests that there is less steric hindrance between the ferrocenylphosphine ligands than between the carbonyl ligands. The P–Cr–P bond angles increase from 85.7(1)° in **2a** to 87.26(3)° in **3a**. The Cr–P–C bond angles also become more obtuse, increasing from 122.49(4)° in **1a** to 123.8(3)° (average) in **2a** and finally to 125.87(7)° in **3a**. Likewise, the P–Mo–P (86.83(2)° (**3b**), 84.85(4)° (**2b**)) and Mo–P–C (125.34(8)° (**3b**), 123.5(2)° (**2b**)) (average) bond angles in **3b** increase compared to **2b**. The P–Mo–P bond angle in *cis*-[Mo(CO)₄(PH₂Ph)₂]²⁵ is 87.9(1)°, as opposed to the more acute angle of 84.85(4)° in **2b**. The M–P–C_{Fc} bond angles are large and very similar for all complexes (122.49(4) and 121.69(9)° in **1a** and **1c** and slightly larger in **2a–c** (122.6(3) to 124.8(3)°) and **3a,c** (125.87(7) and 125.34(8)°). In comparison, the Mo–P–C bond angles in *cis*-[Mo(CO)₄(PH₂Ph)₂] are more acute (120.6(1)°) compared to **2b**. The P–C_{Fc} bond lengths of **1a–c** and **2a–c** are also very similar (*ca.* 180 pm) as are the ferrocenyl moieties in these complexes.

However, the bond lengths around the metal atom differ greatly between the complexes, as expected from the larger differences in atomic radii. For example, the Cr–P bond length of **1a** is 236.30(3) pm, and the W–P bond length of **1c** is 251.12(8) pm. The Cr–P and W–P bond lengths of **2a** and **2c** are shorter than those of **1a** and **1c**. This is again due the second FcPH₂ ligand. The Cr–P bond lengths remain relatively constant at 236.30(3) pm in **1a**, 234.4(3) and 235.0(3) pm in **2a** and 235.15(6) pm in **3a**. The Mo–P bond in **3b** increases insignificantly to 250.57(7) pm from 250.3(1) pm in **2b**. Likewise, the Mo–P bond lengths of *cis*-[Mo(CO)₄(PH₂Ph)₂] and *fac*-[Mo(CO)₃(PH₂Ph)₃] do not change at 250.8(3) and 249.8(3) pm, respectively.²⁵

The average Cr–C bond length of **1a** is 189.1(1) pm with the shortest bond (186.4(1) pm) *trans* to phosphorus. Bond lengths of **1c** follow the same trend but are longer (average W–C bond



length is 203.6(3) pm with the shortest bond (201.0(3) pm *trans* to phosphorus). The bond lengths around the Cr and W atoms of **2a** and **2c** are shorter than those of **1a** and **1c** (**2a**: average Cr–C 186.9(1) pm; **2c**: W–C average 199.7(1) pm). The same trend is observed in **2b** which has an average Mo–C bond length of 200.7(6) pm (Mo–C 202.0(1) pm in $[M(CO)_4(PH_2Ph)_2]^{25}$) and for **3a,b** (**3a**: Cr–C 184.9(2) pm; **3b**: Mo–C 198.0(3) pm). This shortening can be attributed to increased back-bonding between the metal centre and carbonyl ligands and is supported by a decrease in the A_1 mode of the CO stretching vibration (Table 1). This correlation was also observed for the phenylphosphine complexes $[M(CO)_4(PH_2Ph)_2]$ and $[M(CO)_3(PH_2Ph)_3]$ ($M = Cr, Mo, W$).²⁵

Hydrophosphination

The addition of P–H bonds to C–C double or triple bonds (hydrophosphination reaction) is a very versatile way of synthesising new phosphines.^{3,26} After seminal work on catalytic hydrophosphination,^{26g,h} renewed activity in this area was observed recently.^{26i–k} Therefore, the ability of the coordinated ferrocenylphosphine to undergo hydrophosphination reactions was tested by screening **1c** with a number of alkene substrates. KO*t*Bu (10 mol%) was used to catalyse the hydrophosphination reactions, and dry THF was employed as the reaction medium to allow for sufficient solubility of all reaction components. The general procedure involved mixing **1c** with KO*t*Bu in THF followed by addition of one equivalent of one of the alkene substrates, all of which are liquids, after which the mixture was heated to reflux for several hours. Subsequent analysis of the reaction mixture by $^{31}P\{^1H\}$ NMR spectroscopy showed that alkenes bearing an electron-donating group (EDG), that is, styrene and cyclopentene, did not undergo hydrophosphination even when refluxing was continued for 24 h. However, alkenes with an electron-withdrawing group (EWG) did undergo hydrophosphination, and the stronger the EWG effect the faster the reaction. Thus, hydrophosphination of acrylonitrile, which bears a strong EWG, was complete after 5 h, while that of methyl acrylate, containing a weak EWG, took 20 h. The products $[W(CO)_5\{PH(Fe)(CH_2CH_2CN)\}]$ (**4a**) and $[W(CO)_5\{PH(Fe)(CH_2CH_2C(O)OMe)\}]$ (**4b**) were purified by column chromatography (they are eluted considerably more slowly than **1c**) and fully characterised (Scheme 4).

The 1H , $^{31}P\{^1H\}$ and ^{31}P NMR spectra confirm the anti-Markovnikov addition of the P–H bond across the C–C double

bond of the alkene substrate. In the 1H NMR spectrum, the signal of the P–H protons of **4a** and **4b** is shifted downfield (5.87 or 5.76 ppm, respectively) compared to **1c** (5.65 ppm) with a large ^{31}P – 1H coupling of 344 Hz, a slight increase from 342 Hz in **1c**, but appears as a doublet of triplets due to the $^3J_{HH}$ coupling of 4 or 5.4 Hz with the two methylene protons of the new cyanoethyl or methoxycarbonyl ethyl substituent. Likewise, a doublet with a large downfield shift to –45.4 ppm (**4a**, $^1J_{PH} = 345$ Hz) or –42.6 ppm (**4b**, $^1J_{PH} = 343$ Hz) from –101.8 ppm in **1c** is observed in the ^{31}P NMR spectrum. The IR spectra of **4a,b** show some similarity to that of **1c**. The carbonyl stretching frequencies are unchanged at 2073 and 2071 cm^{-1} , respectively. The carbonyl stretching band of the carboxylate moiety of **4b** was observed at 1738 cm^{-1} , but no nitrile stretching band was observed for **4a**.

The distorted octahedral environment ($87.8(1)^\circ$ to $94.2(1)^\circ$) and the bond lengths around the tungsten atom in **4a** (Fig. 4) change only slightly compared to **1c** (W–P 252.0(8) vs. 251.1(8) pm in **1c**). The average W–C bond length is 202.4(4) pm (*cf.* 203.6(3) pm in **1c**). The shortest W–C bond (197.9(4) pm) is again that *trans* to phosphorus, which is 3.1 pm shorter than that in **1c**. These very small changes in bond lengths indicate that there is no significant change in the coordination properties, which would otherwise be expected when moving from a primary to secondary phosphine. The phosphorus atom exhibits a distorted tetrahedral environment with large $W-P-C_{Fc}$ and $W-P-C_{Et}$ bond angles ($121.7(1)^\circ$ and $110.7(1)^\circ$, respectively) and a small $C_{Fc}-P-C_{Et}$ bond angle ($104.0(2)^\circ$).

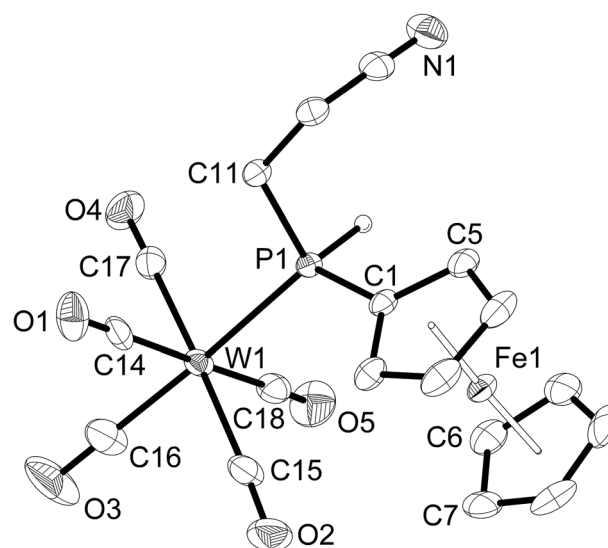
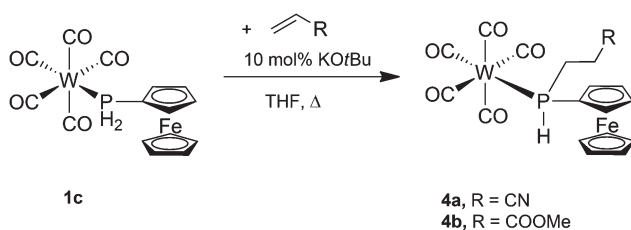
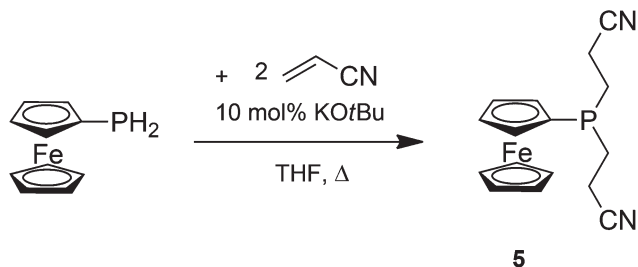


Fig. 4 Molecular structure of $[W(CO)_5\{PH(Fe)(CH_2CH_2CN)\}]$ (**4a**). Hydrogen atoms other than P–H are omitted for clarity. Ellipsoids drawn at 50% probability. Selected bond lengths (pm) and bond angles ($^\circ$): W(1)–C(16) 197.9(4), W(1)–C(18) 202.1(5), W(1)–C(15) 203.7(4), W(1)–C(14) 203.8(5), W(1)–C(17) 204.5(4), W(1)–P(1) 252.04(8), P(1)–C(1) 178.4(3), P(1)–C(11) 183.2(3), C(16)–W(1)–P(1) 175.8(2), C(18)–W(1)–P(1) 93.2(1), C(15)–W(1)–P(1) 94.2(1), C(14)–W(1)–P(1) 87.8(1), C(17)–W(1)–P(1) 90.6(1), C(1)–P(1)–C(11) 104.0(2), C(1)–P(1)–W(1) 121.7(1), C(11)–P(1)–W(1) 110.7(1), C(12)–C(11)–P(1) 118.3(2).



Scheme 4 Synthesis of $[W(CO)_5\{PH(Fe)(CH_2CH_2CN)\}]$ (**4a**) and $[W(CO)_5\{PH(Fe)(CH_2CH_2C(O)OMe)\}]$ (**4b**).





Scheme 5 Synthesis of $\text{FcP}(\text{CH}_2\text{CH}_2\text{CN})_2$ (**5**).

FcPH_2 undergoes a similar hydrophosphination reaction as **1c**; however, the di-hydrophosphination product, the tertiary phosphine $\text{FcP}(\text{CH}_2\text{CH}_2\text{CN})_2$ (**5**), is observed even with only one equivalent of acrylonitrile in refluxing THF and a catalytic amount of KOtBu (Scheme 5). **5** is obtained in a better yield when two equivalents of acrylonitrile are employed. **5** was isolated as a viscous orange oil by column chromatography under an inert atmosphere, since it is rapidly oxidised upon exposure to air.

In the ^{31}P NMR spectrum, the signal of the phosphorus atom of **5** is shifted downfield to -74.4 ppm compared to FcPH_2 (-144.2 ppm). This signal is still significantly upfield from those of the related compounds $\text{FcCH}_2\text{P}(\text{CH}_2\text{CH}_2\text{CN})_2$ (-22.1 ppm)²⁷ and $\text{PhP}(\text{CH}_2\text{CH}_2\text{CN})_2$ (-23.8 ppm).²⁸ The $^{13}\text{C}\{^1\text{H}\}$ NMR spectrum of **5** reveals an increase in the $^{13}\text{C}-^{31}\text{P}$ coupling constants compared with FcPH_2 . The signal of the *ipso* carbon atom shifts downfield to 68.1 ppm from 64.1 ppm in FcPH_2 with similar $^1J_{\text{CP}}$ values (5.0 Hz in FcPH_2 , 5.1 Hz in **5**). Likewise, the signal of the *meta* carbon atom is shifted downfield to 71.2 ppm with an increased $^{13}\text{C}-^{31}\text{P}$ coupling constant of 10.1 Hz compared with 4.0 Hz in FcPH_2 .

Conclusions

The mono-, bis- and tris-ferrocenylphosphine complexes $[\text{M}(\text{CO})_5(\text{PH}_2\text{Fc})]$ (**1a-c**), $[\text{M}(\text{CO})_4(\text{PH}_2\text{Fc})_2]$ (**2a-c**) and $[\text{M}(\text{CO})_3(\text{PH}_2\text{Fc})_3]$ (**3a-c**) with $\text{M} = \text{Cr}, \text{Mo}, \text{W}$ are readily available from FcPH_2 and suitable metal carbonyl complexes. The molecular structures of **1a,c**, **2a-c** and **3a,b** and a comparison of the X-ray structural and spectroscopic data of **2b** and **3b** with those of the known phenylphosphine complexes *cis*- $[\text{Mo}(\text{CO})_4(\text{PH}_2\text{Ph})_2]$ and *fac*- $[\text{Mo}(\text{CO})_3(\text{PH}_2\text{Ph})_3]$ reveal that FcPH_2 exerts similar steric effects on the complex as PhPH_2 , but its electronic behaviour is significantly different. By comparing the carbonyl stretching frequencies of the complexes, it can be concluded that FcPH_2 is as good a σ donor as PhPH_2 .

The coordinated FcPH_2 ligand of **1c** undergoes hydrophosphination in the presence of catalytic amounts of KOtBu with alkene substrates bearing EWGs, such as acrylonitrile and methyl acrylate, yielding the secondary phosphine complexes $[\text{W}(\text{CO})_5\{\text{PH}(\text{Fc})(\text{CH}_2\text{CH}_2\text{CN})\}]$ (**4a**) and $[\text{W}(\text{CO})_5\{\text{PH}(\text{Fc})(\text{CH}_2\text{CH}_2\text{C}(\text{O})\text{OMe})\}]$ (**4b**). Extending this method to the free ferrocenylphosphine yielded $\text{FcP}(\text{CH}_2\text{CH}_2\text{CN})_2$ (**5**).

The findings presented above show that FcPH_2 is a versatile ligand that behaves and interacts much like the far more difficult to handle PhPH_2 , and it also contains a useful redox-active ferrocenyl moiety.

Experimental

General methods

Preparation of all compounds was carried out under an N_2 atmosphere using standard vacuum-line and Schlenk techniques. All reactions were performed at ambient temperature and pressure unless otherwise stated. Where necessary, solvents were degassed using the standard freeze-pump-thaw method.²⁹ The drying and distillation of solvents was conducted according to literature methods²⁹ or solvents were dried with an MB SPS-800 Solvent Purification System. $[\text{M}(\text{CO})_5(\text{thf})]$ ($\text{M} = \text{Cr}, \text{Mo}, \text{W}$),²¹ $[\text{M}(\text{CO})_4(\text{L})]$ ($\text{M} = \text{Cr}, \text{Mo}, \text{L} = \text{nbid}; \text{M} = \text{W}, \text{L} = \text{tmpa}$) ($\text{nbid} = 2,5\text{-norbornadiene}; \text{tmpa} = N,N,N',N'\text{-tetramethyl-1,3-propanediamine}$),²² $[\text{M}(\text{CO})_3(\text{L})_3]$ ($\text{M} = \text{Mo}, \text{Cr}, \text{L} = \text{MeCN}; \text{M} = \text{W}, \text{L} = \text{EtCN}$),²¹ and FcPH_2 ³ were prepared according to literature methods. $\text{Cr}(\text{CO})_6$ (Roth), $\text{Mo}(\text{CO})_6$ and $\text{W}(\text{CO})_6$ (Acros) were used as supplied without further purification. Silica gel 60A (Acros) was used as the stationary phase for column chromatography. Mass spectra were obtained in ESI mode with a BRUKER Daltonics FT-ICR-MS spectrometer (Type APEX II, 7 Tesla). Elemental analysis was performed with a Heraeus VARIO EL Analyser. IR spectra ($4000\text{--}400\text{ cm}^{-1}$) were recorded as Nujol mulls with a PerkinElmer Spectrum 2000 FT-IR spectrometer. ^1H , $^{13}\text{C}\{^1\text{H}\}$, $^{31}\text{P}\{^1\text{H}\}$ and ^{31}P NMR spectra were recorded with a Bruker AVANCE DRX 400 MHz instrument at $25\text{ }^\circ\text{C}$. Chemical shifts δ of ^1H , ^{13}C , ^{31}P are reported in parts per million (ppm) at 400.12, 100.63 and 162.02 MHz, respectively. ^1H NMR spectra were referenced to TMS (0.00 ppm) or the protic impurity solvent signals in the solvent CDCl_3 (7.26 ppm). ^{13}C NMR spectra were referenced to the solvent signal, CDCl_3 (77.16 ppm). $^{13}\text{C}\{^1\text{H}\}$ and $^{31}\text{P}\{^1\text{H}\}$ experiments were referenced to TMS on the Ξ scale.³⁰ ^{31}P NMR experiments were referenced to 85% H_3PO_4 as external standard. Coupling constants of higher spin systems were determined by using the NMR software MestReNova 8 (Mestrelab Research).³¹

Synthesis and characterisation

$\text{Fe}(\eta^5\text{-C}_5\text{H}_4\text{PH}_2)(\eta^5\text{-C}_5\text{H}_5)$ (FcPH_2). This is a modification of the method reported previously.¹² A solution of $\text{FcP}(\text{O})(\text{OEt})_2$ (5.0 g, 15.5 mmol) in diethyl ether (*ca.* 10 mL) was added to LiAlH_4 (0.59 g, 15.5 mmol) in diethyl ether (*ca.* 20 mL) with stirring at *ca.* $-70\text{ }^\circ\text{C}$. This mixture was warmed to room temperature and left to stir overnight (14–20 h). Unconsumed LiAlH_4 was carefully hydrolysed with distilled water while the mixture was cooled over ice. The orange organic phase was separated and dried over anhydrous MgSO_4 . After reducing the volume to *ca.* 2–3 mL the crude product was purified by column chromatography on silica gel with CH_2Cl_2 as eluent.



The resulting viscous orange oil was still contaminated with ferrocene, which was removed by sublimation (36 °C, 10⁻³ mbar) over several hours. Additional purification can be achieved by sublimation of the product, FcPH₂, at 30 °C under high vacuum (10⁻⁶ mbar). Yield = 3.22 g, 55%. FcPH₂ has already been described in the literature. However, the NMR data are presented here for easy reference. ¹H NMR (CDCl₃): δ = 3.81 (d, 2H, ¹J_{HP} = 203.6 Hz, PH₂), 4.16 (s, 5H, C₅H₅), 4.25 (s, 2H, C₅H₄), 4.27 (s, 2H, C₅H₄); ¹³C{¹H} NMR (CDCl₃): δ = 64.1 (d, ¹J_{CP} = 5.0 Hz, *ipso*-C in C₅H₄), 69.3 (s, C₅H₅), 70.7 (d, ³J_{CP} = 4.0 Hz, *m*-C in C₅H₄), 75.7 (d, ²J_{CP} = 13.8 Hz, *o*-C in C₅H₄); ³¹P NMR (CDCl₃): δ = -144.2 (t, ¹J_{PH} = 203.6 Hz, PH₂).

[M(CO)₅(PH₂Fc)] (1a, M = Cr; 1b, M = Mo; 1c, M = W). A solution of M(CO)₆ in THF (*ca.* 50 mL) was irradiated with a Hg vapour lamp for 3 h at room temperature to generate [M(CO)₅(thf)] (M = Cr, Mo, W). This solution was then added immediately to an equimolar amount of FcPH₂ in THF (*ca.* 10 mL) and the mixture was stirred overnight at room temperature. An orange residue containing the product was obtained after all solvent and volatiles were evaporated under reduced pressure. This residue was dissolved in a minimal volume of CH₂Cl₂ (*ca.* 2 mL) and passed through a silica gel column with CH₂Cl₂/*n*-hexane (30:70) as eluent. The orange band corresponding to the product was collected and the solvent evaporated under reduced pressure to obtain [M(CO)₅(PH₂Fc)] as an orange powder of high purity. Any remaining FcPH₂ and/or M(CO)₆ in the product was removed by sublimation under high vacuum (10⁻³ mbar). Yields: **1a** 30%, **1b** 44%, **1c** 52%.

1a: ¹H NMR (CDCl₃): δ = 4.16 (s, 5H, Fe-C₅H₅), 4.35 (s, 4H, Fe-C₅H₄), 5.27 (d, ¹J_{HP} = 333.9 Hz, 2H, PH₂); ¹³C{¹H} NMR (CDCl₃): δ = 64.5 (d, ¹J_{CP} = 45.7 Hz, *ipso*-C in C₅H₄), 69.8 (s, C₅H₅), 71.5 (d, ³J_{CP} = 7.7 Hz, *m*-C in C₅H₄), 73.9 (d, ²J_{CP} = 12.2 Hz, *o*-C in C₅H₄), 216.1 (d, ²J_{CP} = 13.7 Hz, CO *eq*), 220.4 (d, ²J_{CP} = 7.3 Hz, CO *ax*); ³¹P NMR (CDCl₃): δ = -47.5 (t, ¹J_{PH} = 333.9 Hz, PH₂); IR (Nujol, cm⁻¹): 2066w (CO), 1946m (CO), 1931s (CO), 1917vs (CO); MS ESI pos., CH₂Cl₂/MeOH, *m/z* = 431.89 [M + Na]⁺; elemental analysis calcd (%) for C₁₅H₁₁CrFeO₅P: C 43.94, H 2.70; found: C 44.05, H 2.68.

1b: ¹H NMR (CDCl₃): δ = 4.24 (s, 5H, Fe-C₅H₅), 4.40 (m, 2H, Fe-C₅H₄), 4.42 (m, 2H, Fe-C₅H₄), 5.31 (d, ¹J_{HP} = 328.0 Hz, 2H, PH₂); ¹³C{¹H} NMR (CDCl₃): δ = 63.7 (d, ¹J_{CP} = 45.9 Hz, *ipso*-C in C₅H₄), 69.9 (s, C₅H₅), 71.8 (d, ³J_{CP} = 7.7 Hz, *m*-C in C₅H₄), 74.7 (d, ²J_{CP} = 13.2 Hz, *o*-C in C₅H₄), 205.0 (d, ²J_{CP} = 9.2 Hz, CO *eq*), 208.8 (d, ²J_{CP} = 23.7 Hz, CO *ax*); ³¹P NMR (CDCl₃): δ = -81.5 (t, ¹J_{PH} = 328.0 Hz, PH₂); IR (Nujol, cm⁻¹): 2074w (CO), 1950s (CO), 1933s (CO), 1921vs (CO); MS ESI pos., CH₂Cl₂/MeOH, *m/z* = 477.86 [M + Na]⁺; elemental analysis calcd (%) for C₁₅H₁₁FeMoO₅P: C 39.68, H 2.44; found: C 39.59, H 2.40.

1c: ¹H NMR (CDCl₃): δ = 4.25 (s, 5H, Fe-C₅H₅), 4.42 (m, 2H, Fe-C₅H₄), 4.46 (m, 2H, Fe-C₅H₄), 5.65 (d, ¹J_{HP} = 341.5 Hz, 2H, PH₂); ¹³C{¹H} NMR (CDCl₃): δ = 63.5 (d, ¹J_{CP} = 51.9 Hz, *ipso*-C in C₅H₄), 70.0 (s, C₅H₅), 71.9 (d, ³J_{CP} = 8.1 Hz, *m*-C in C₅H₄), 74.6 (d, ²J_{CP} = 13.2 Hz, *o*-C in C₅H₄), 195.9 (d, ²J_{CP} = 7.1 Hz, CO *eq*), 198.1 (d, ²J_{CP} = 22.2 Hz, CO *ax*); ³¹P NMR (CDCl₃): δ = -101.8 (t with ¹⁸³W satellites, ¹J_{PH} = 341.5 Hz, ¹J_{PW} = 221.0 Hz, PH₂); IR (Nujol, cm⁻¹): 2073w (CO), 1935vs (CO), 1916vs (CO),

1898s (CO); MS ESI pos., CH₂Cl₂/MeOH, *m/z* = 563.90 [M + Na]⁺; elemental analysis calcd (%) for C₁₅H₁₁FeO₅PW: C 33.25; H 2.05; found: C 33.30; H 1.99.

cis-[M(CO)₄(PH₂Fc)₂] (2a, M = Cr; 2b, M = Mo; 2c, M = W). A solution containing two equivalents of FcPH₂ in toluene (5.0 mL) was added to a solution of [M(CO)₄(L)] (M = Cr or Mo, L = nbd; M = W, L = tmpa) in toluene (*ca.* 10 mL) at room temperature. The mixture was stirred overnight at room temperature or, in the case of **2c**, heated to 60 °C. The solvent and volatiles were then removed under high vacuum (10⁻³ mbar). The remaining orange residue was dissolved in a minimal volume of CH₂Cl₂ (*ca.* 2 mL) and passed through a silica gel column with CH₂Cl₂/*n*-hexane (1:1) as eluent. The orange band corresponding to the product was collected and the solvent evaporated under reduced pressure until pale orange crystals of pure *cis*-[M(CO)₄(PH₂Fc)₂] formed. The crystals were isolated by filtration, washed with *n*-hexane (3 × 10 mL) and dried under vacuum. Yields: **2a** 59%, **2b** 58%, **2c** 69%.

2a: ¹H NMR (CDCl₃): δ = 4.22 (s, 10H, Fe-C₅H₅), 4.38 (br s, 4H, Fe-C₅H₄), 4.41 (br s, 4H, Fe-C₅H₄), 5.23 (m, ¹J_{HP} = 333.1 Hz, ³J_{HP} = 13.0 Hz, 4H, PH₂, AA'X₂X'₂ spin system, simulated³¹ (see ESI[†])); ¹³C{¹H} NMR (CDCl₃): δ = 65.9 (t, ¹J_{CP} = 49.5 Hz, ³J_{CP} = 25.3 Hz, *ipso*-C in C₅H₄), 69.9 (s, C₅H₅), 71.3 (t, ³J_{CP} = 7.1 Hz, ⁵J_{CP} = 3.3 Hz, *m*-C in C₅H₄), 74.0 (t, ²J_{CP} = 11.1 Hz, ⁴J_{CP} = 5.6 Hz, *o*-C in C₅H₄), 220.1 (t, ²J_{CP} = 14.4 Hz, CO *cis*), 226.0 (d, ²J_{CP} = 9.3 Hz, CO *trans*); ³¹P NMR (CDCl₃): δ = -36.3 (m, ¹J_{PH} = 333.1 Hz, ²J_{PP} = -29.0 Hz, PH₂, AA'X₂X'₂ spin system, simulated³¹ (see ESI[†])); IR (Nujol, cm⁻¹): 2018w (CO), 1922s (CO), 1901s (CO), 1870vs (CO); MS ESI pos., CH₂Cl₂/MeOH, *m/z* = 622.9 [M + Na]⁺; elemental analysis calcd (%) for C₂₄H₂₂CrFe₂O₄P₂: C 48.04, H 3.70; found: C 47.93, H 3.61.

2b: ¹H NMR (CDCl₃): δ = 4.24 (s, 10H, Fe-C₅H₅), 4.40 (br s, 4H, Fe-C₅H₄), 4.42 (br s, 4H, Fe-C₅H₄), 5.22 (m, ¹J_{HP} = 327.0 Hz, ³J_{HP} = 11.0 Hz, 4H, PH₂, AA'X₂X'₂ spin system); ¹³C{¹H} NMR (CDCl₃): δ = 64.8 (t, ¹J_{CP} = 48.5 Hz, ³J_{CP} = 24.2 Hz, *ipso*-C in C₅H₄), 69.9 (s, C₅H₅), 71.5 (t, ³J_{CP} = 7.1 Hz, ⁵J_{CP} = 3.5 Hz, *m*-C in C₅H₄), 74.7 (t, ²J_{CP} = 12.1 Hz, ⁴J_{CP} = 6.1 Hz, *o*-C in C₅H₄), 208.1 (t, ²J_{CP} = 9.5 Hz, CO *cis*), 214.1 (d, ²J_{CP} = 9.3 Hz, CO *trans*); ³¹P NMR (CDCl₃): δ = -72.4 (m, ¹J_{PH} = 326.4 Hz, ²J_{PP} = -17.0 Hz, PH₂, AA'X₂X'₂ spin system); IR (Nujol, cm⁻¹): 2024w (CO), 1901vs (CO), 1879s (CO); MS ESI pos., CH₂Cl₂/MeOH, *m/z* = 668.8 [M + Na]⁺; elemental analysis calcd (%) for C₂₄H₂₂Fe₂MoO₄P₂: C 44.76, H 3.44; found: C 44.74, H 3.50.

2c: ¹H NMR (CDCl₃): δ = 4.25 (s, 10H, Fe-C₅H₅), 4.46 (s, 8H, Fe-C₅H₄), 5.53 (m, ¹J_{HP} = 328.0 Hz, ³J_{HP} = 12.0 Hz, 4H, PH₂, AA'X₂X'₂ spin system); ¹³C{¹H} NMR (CDCl₃): δ = 64.6 (m, ¹J_{CP} = 50.6 Hz, ³J_{CP} = 26.3 Hz, *ipso*-C in C₅H₄), 69.9 (s, C₅H₅), 71.6 (p, ³J_{CP} = 8.1 Hz, ⁵J_{CP} = 4.0 Hz, *m*-C in C₅H₄), 74.6 (t, ²J_{CP} = 12.1 Hz, ⁴J_{CP} = 6.1 Hz, *o*-C in C₅H₄), 200.0 (t, ²J_{CP} = 7.3 Hz, CO *cis*), 204.3 (m, CO *trans*); ³¹P NMR (CDCl₃): δ = -94.2 (m, ¹J_{PH} = 328.0 Hz, ²J_{PP} = -11.0 Hz, ¹J_{WP} = 214.9 Hz, PH₂, AA'X₂X'₂ spin system); IR (Nujol, cm⁻¹): 2025w (CO), 1922s (CO), 1898s (CO), 1865vs (CO); MS ESI pos., CH₂Cl₂/MeOH, *m/z* = 754.9 [M + Na]⁺; elemental analysis calcd (%) for C₂₄H₂₂Fe₂O₄P₂W: C 39.38, H 3.03; found: C 39.35, H 2.86.



leave pure $\text{FcP}(\text{CH}_2\text{CH}_2\text{CN})_2$ as an oily orange solid. Yield: 0.52 g, 70%.

^1H NMR (CDCl_3): δ = 1.78 (m, 4H, $\text{CH}_2\text{CH}_2\text{CN}$), 2.36 (br, 4H, $\text{CH}_2\text{CH}_2\text{CN}$), 4.13 (s, 5H, $\text{Fe}-\text{C}_5\text{H}_5$), 4.18 (br, 2H, $\text{Fe}-\text{C}_5\text{H}_4$), 4.27 (s, 2H, $\text{Fe}-\text{C}_5\text{H}_4$); $^{13}\text{C}\{^1\text{H}\}$ NMR (CDCl_3): δ = 16.5 (d, $^2J_{\text{CP}}$ = 7.4 Hz, CH_2CN), 20.5 (d, $^1J_{\text{CP}}$ = 15.1 Hz, PCH_2), 68.1 (d, $^1J_{\text{CP}}$ = 5.1 Hz, *ipso*-C in C_5H_4), 69.0 (s, C_5H_5), 71.2 (s, *m*-C in C_5H_4), 74.6 (d, $^2J_{\text{CP}}$ = 13.4 Hz, *o*-C in C_5H_4), 119.3 (s, CH_2CN); ^{31}P NMR (CDCl_3): δ = -74.4 (s); MS ESI pos., $\text{CH}_2\text{Cl}_2/\text{MeOH}$, m/z = 325.06 $[\text{M} + \text{H}]^+$.

Crystal structure determinations

The data were collected on a Gemini area detector diffractometer (Rigaku Inc.) using Mo-K α radiation (λ = 71.073 pm) and ω -scan rotation. Data reduction was performed with CrysAlis-Pro³² including the program SCALE3 ABSPACK for empirical absorption correction. The structures of **1a,c**, **2a-c** and **3a,b** were solved by direct methods and that of **4a** was solved with Patterson methods with SHELXS-97³³ or SIR92.³⁴ The refinement was performed with SHELXL-97.³³ As a result of the extremely small and moderately diffracting crystal (small needle), the carbon atoms of **2c** were refined isotropically. The non-hydrogen atoms of all other structures were refined with anisotropic thermal parameters. A difference-density Fourier map was used to locate all hydrogen atoms of **1a** and **1c**, whereas H atoms of all other structures were calculated on idealised positions by using the riding model. The structures **1a** and **1c** are isostructural. This is also the case for the series **2a-c** and **3a,b** (see Table S1, ESI[†]). Structure figures were generated with ORTEP³⁵ and DIAMOND-3.³⁶ CCDC 1420127 (**1a**), 1420128 (**1c**), 1420129 (**2a**), 1420130 (**2b**), 1420131 (**2c**), 1420132 (**3a**), 1420133 (**3b**) and 1420134 (**4a**) contain the supplementary crystallographic data for this paper.

Acknowledgements

We gratefully acknowledge financial support from by the European Union and the Free State of Saxony (Landesinnovationspromotion for J. P. S.) and the Graduate School Leipzig School of Natural Sciences – Building with Molecules and Nano-objects (BuildMoNa).

References

- (a) T. B. Rauchfuss, in *Homogeneous Catalysis with Metal Phosphine Complexes*, ed. L. H. Pignolet, Plenum Press, New York, 1993, ch. 7; (b) *Phosphorus(III) Ligands in Homogeneous Catalysis: Design and Synthesis*, ed. P. C. Kamer and P. W. N. M. van Leeuwen, John Wiley & Sons Ltd., UK, 2012; (c) A. Behr and P. Neubert, *Applied Homogeneous Catalysis*, Wiley-VCH Verlag & Co. KGaA, 2012.
- D. E. C. Corbridge, *Phosphorus: Chemistry, Biochemistry and Technology*, CRC Press, Taylor & Francis Group, Boca Raton, FL, 6th edn, 2013.
- J. T. Fleming and L. J. Higham, *Coord. Chem. Rev.*, 2015, **297–298**, 127.
- W. Henderson and S. R. Alley, *J. Organomet. Chem.*, 2002, **656**, 120.
- N. J. Goodwin, W. Henderson, B. K. Nicholson, J. Fawcett and D. R. Russell, *J. Chem. Soc., Dalton Trans.*, 1999, 1785.
- N. J. Goodwin, W. Henderson and B. K. Nicholson, *Chem. Commun.*, 1997, 31.
- P. P. Power, R. A. Bartlett, M. M. Olmstead and G. A. Sigel, *Inorg. Chem.*, 1987, **26**, 1941.
- P. P. Power, B. Twamley, C. Hwang and N. J. Hardman, *J. Organomet. Chem.*, 2000, **609**, 152.
- K. V. Katti, K. R. Prabhu, N. Pillarsetty and H. Gali, *J. Am. Chem. Soc.*, 2000, **122**, 1554.
- R. M. Hiney, L. J. Higham, H. Müller-Bunz and D. G. Gilheany, *Angew. Chem.*, 2006, **118**, 7406, (*Angew. Chem. Int. Ed.*, 2006, **45**, 7248).
- (a) P. Štěpnička, *Ferrocenes. Ligands, Materials and Biomolecules*, John Wiley & Sons Ltd., West Sussex, 2008; (b) A. Togni and T. Hayashi, *Ferrocenes. Homogeneous Catalysis. Organic Synthesis. Material Science*, VCH, New York, Weinheim, 1995.
- S. Tschirschwitz, P. Lönnecke and E. Hey-Hawkins, *J. Chem. Soc., Dalton Trans.*, 2007, 1377.
- C. Spang, F. T. Edlmann, M. Noltemeyer and H. W. Roesky, *Chem. Ber.*, 1989, **122**, 1247.
- R. Kalio, P. Lönnecke and E. Hey-Hawkins, *J. Organomet. Chem.*, 2008, **693**, 590.
- R. Kalio, P. Lönnecke, A. Cinquantini, P. Zanello and E. Hey-Hawkins, *Z. Anorg. Allg. Chem.*, 2007, **633**, 2470.
- S. I. M. Paris, F. R. Lemke, R. Sommer, P. Lönnecke and E. Hey-Hawkins, *J. Organomet. Chem.*, 2005, **690**, 1807.
- S. I. M. Paris, J. L. Petersen, E. Hey-Hawkins and M. P. Jensen, *Inorg. Chem.*, 2006, **45**, 5561.
- R. Sommer, P. Lönnecke, P. K. Baker and E. Hey-Hawkins, *Inorg. Chem. Commun.*, 2002, **5**, 115.
- R. Sommer, P. Lönnecke, J. Reinhold, P. K. Baker and E. Hey-Hawkins, *Organometallics*, 2005, **24**, 5256.
- J. Svava, N. Weferling and T. Hofmann, Phosphorus Compounds, Organic, in *Ullmann's Encyclopedia of Industrial Chemistry*, John Wiley & Sons, Inc, 2008.
- W. A. Herrmann and A. Salzer, *Synthetic Methods of Organometallic and Inorganic Chemistry*, Thieme, New York, 1996, vol. 1.
- J. C. Kotz, C. L. Nivert, J. M. Lieber and R. C. Reed, *J. Organomet. Chem.*, 1975, **84**, 255.
- O. Köhl, *Phosphorus-31 NMR Spectroscopy: A Concise Introduction for the Synthetic Organic and Organometallic Chemist*, Springer, 2008.
- R. H. Crabtree, *The Organometallic Chemistry of the Transition Metals*, John Wiley & Sons, Inc., New Jersey, 5th edn, 2009.
- T. Campbell, A. M. Gibson, R. Hart, S. D. Orchard, S. J. A. Pope and G. Reid, *J. Organomet. Chem.*, 1999, **592**, 296.



